ELSEVIER

Synthesis, characterization and structure of diiron organometallic derivatives of 2,9-dimethyl-1,10-dihydro-dicyclopenta[a,h]naphthalene

M.K. Amshumali [a], Ivonne Chávez [a], Verónica Arancibia [a], F. Burgos O [a], Juan M. Manríquez [a,*], Elies Molins [b,*], Anna Roig [b]

[a] *Departamento de Química Inorgánica, Facultad de Química, Pontificia Universidad Católica de Chile, Vicua Mackena 4860, Casilla306, Correo22, Santiago de Chile, Chile*
[b] *Institut de Ciència de Materials de Barcelona (CSIC) Campus UAB, 08193 Bellaterra, Barcelona, España*

Abstract

A new fused ring compound 2,9-dimethyl-1,10-dihydro-dicyclopenta[a,h]naphthalene (**VI**), (H$_2$L), has been synthesized from naphthalic anhydride. Two organometallic binuclear complexes, [Cp*Fe-L-FeCp*] (**1**) and the mixed valence compound, [Cp*Fe-L-FeCp*]$^+$BF$_4^-$ (**2**) have been characterized by spectroscopic and electrochemical techniques. The structure resolution of (**1**) by single crystal X-ray diffraction shows that the two organometallic fragments Cp*Fe are in an *anti* position. Cyclic voltammetry exhibits a potential difference of 348 mV between both redox peaks. The Mössbauer investigation at different temperatures shows a uniform environment for the neutral compound (**1**) and two sites, assigned to Fe^{2+} and Fe^{3+} for the compound (**2**). The information gathered by all the previously mentioned techniques indicates that the studied binuclear complex belongs to the mixed valence class II complexes according to the classification of Robin and Day.
© 2004 Elsevier B.V. All rights reserved.

Keywords: Binuclear complexes; Dicyclopentanaphthalene; Mixed valence

1. Introduction

In recent years, the synthesis of binuclear transition metal complexes derived from the 4$n\pi$ electron hydrocarbon pentalene and its mono and dibenzologs series have received a renovated interest, with special regard to the electronic interaction between metallic centers [1–10]. For n = 3, the pentalene monobenzolog series has two isomers, s-indacene and as-indacene and it has been found that the geometry of the bridging ligand plays an important role in the extent of delocalization of the mixed valence derivatives. For example, while ESR, Mössbauer, electrochemical and magnetic data for the diiron monocation species [Cp*Fe-s-indacene-FeCp*]$^+$, are consistent with a completely detrapped valence system, the analog monocationic [Cp*Fe-as-indacene-FeCp*]$^+$, for which a relatively localized structure can be drawn, exhibiting a classical trapped ferrocene and ferrocinium centers [6]. For n = 4, the pentalene dibenzologs series, as shown in Fig. 1, consist of four isomers: dicyclopenta[a,f]naphthalene (**A**), dicyclopenta[a,h]naphthalene (**B**), dicyclopenta[a,g]naphthalene (**C**) and dicyclopenta[b,g]naphthalene (**D**). Attempting to understand the relation between geometry of the bridging ligand and distance between the metal centers with the degree
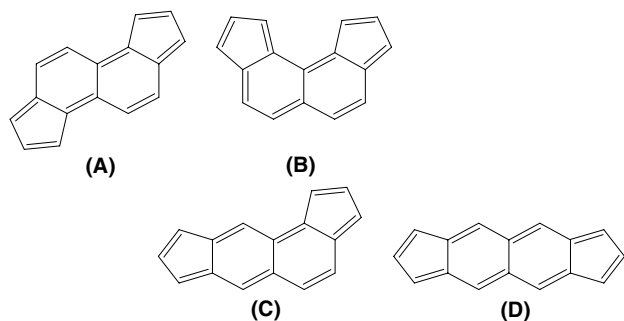
Fig. 1. (**A**) Dicyclopenta[*a,f*]naphthalene; (**B**) dicyclopenta[*a,h*]naphthalene, (**C**) dicyclopenta[*a,g*]naphthalene and (**D**) dicyclopenta[*b,g*]naphthalene.

of electronic interaction, we have undertaken the synthesis of the corresponding binuclear complexes derived from these series. In a previous work, we have reported the preparation and X-ray structure of the biferrocene derivative of isomer **A**, [Cp*Fe-(dicyclopenta[*a,f*]naphthalenylene)-FeCp*], together with the study of the electronic delocalization of its mono-oxidized salt, [Cp*Fe − (dicyclopenta[*a, f*]naphthalenylene)-FeCp*]$^+$BF$_4^-$ [11]. Preliminary studies of bis(ligand)dimetal complexes derivatives of isomer **B** have already been reported by Katz et al. [4], however, the characterization of the neutral diiron species was complicated due to their very low solubility, and the dicationic dicobalt derivative could only be obtained in a very low yield. Here, we describe a high yield synthesis of a substituted dihydro isomer **B**, 2,9-dimethyl-1,10-dihydro-dicyclopenta[*a,h*]naphthalene, the preparation of the corresponding diiron mixed valence derivative and the study of its electronic delocalization.

2. Experimental

2.1. Instrumental

^{1}H and ^{13}C{H} NMR spectra were recorded on Bruker AC-200P (200 and 50 MHz for ^{1}H and ^{13}C, respectively), chemical shifts are reported in ppm relative to TMS. FT-IR spectra were recorded on Bruker Vector-22 spectrophotometer using a nujol mull between KBr disks. NIR spectra were performed on a UV–Vis-NIR SHIMADZU UV-3101 PC scanning spectrophotometer. Elemental analysis were carried out with a Fisons instruments EA-1108 CHNS elemental analyzer.

Cyclic voltammetry measurements were carried out with a Bioanalytical Systems voltammetric analyzer (model CV-50w, version 2.3). The working electrode was Pt or a glassy carbon disk. The auxiliary electrode was a platinum coil electrode, which was isolated from the bulk solution by a glass tube with a small porosity glass frit at the end. Neutro aluminum oxide was placed

on the frit, and the tube was filled with a 0.1 M solution of supporting electrolyte, [N(Bu)$_4$]BF$_4$ (Bu = butyl). The reference electrode was a Ag/AgCl wire placed in a tube with a cracked glass bead at the end and containing aqueous tetramethylammonium chloride. The concentration of this solution was varied until the potential value was 0.0 V versus the saturated calomel electrode (SCE). This electrode was located inside a Luggin capillary in the electrochemical cell. The solvent used was dichloromethane. All the experiments were carried out under argon atmosphere, at room temperature (20 °C).

Mössbauer spectra were obtained using a constant acceleration Mössbauer spectrometer with a ^{57}Co/Rh source. The source was moved via triangular velocity waveform and the γ counts were collected in a 512 multi-channel analyzer. The data were folded, plotted and fitted by a computer procedure. Velocity calibration was performed using 25 μm thick metallic Fe foil. The Mössbauer spectral parameters are given relative to this standard at room temperature. Both X-ray structural studies and Mössbauer analysis were carried out at the ICMAB-CSIC.

2.2. General considerations

All reactions were carried out under nitrogen and in dry solvents. The following materials were used as supplied commercially without further purification; diethyl methyl malonate, KOH, HCl, *n*-butyl lithium (1.6 M) polyphosphoric acid and ethyl alcohol. The reported procedures were followed to synthesize 1,8-dibromomethylnaphthalene from naphthalic anhydride [4] and Cp*Fe(acac) [12].

2.3. Synthesis

2.3.1. 2-[8-(2,2-Bis-ethoxycarbonyl-propyl)-naphthalen-1-ylmethyl]-2- methyl-malonic acid diethyl ester (**I**)

To 75 cm^3 of ethanol in a 250 cm^3 round-bottomed flask was added Na pieces (7.82 g, 0.34 mol) with stirring at room temperature. When all Na was consumed, diethyl methylmalonate (5.8 g, 0.033 mol) was slowly added. After 30 min stirring at room temperature, 1,8-dibromomethyl-naphthalene, (5.2 g 16.6 mmol) was added and the solution heated under reflux for 3 h. The excess of ethanol was distilled and to the residue was added at 0 °C water and diethylether. After stirring and decantation, the two phases were separated. The solvent of the organic phase was removed on a rotary evaporator affording a thick yellow oily liquid **I** (8.2 g, 16.4 mmol). Yield 99%. (Elemental analysis Calc. for C$_{28}$H$_{36}$O$_8$: C, 67.18; H, 7.24. Found: C, 67.30.H, 7.21%.)

^{1}HNMR (CDCl$_3$, ppm) δ 1.15 (t, 9H, CH3) 4.03 (q, 4 H, CH2), 7.30 d, 4H (*ortho* and *para*) 7.71 (t, 2H *meta*).

2.3.2. 2-[8-(2,2-Dicarboxy-propyl)-naphthalen-1-ylmethyl]-2-methyl-malonic acid (II)

To a solution of KOH (50 g, 0.89 mol) in 50 cm^3 of water, placed in a round-bottomed flask with a nitrogen inlet, tetra ester I (7.05 g, 14.1 mmol) was added and re-fluxed until the ester was completely dissolved. This solution was poured into a mixture of water and ice. Then HCl (37%) was added until a pH of 3–4 was reached. The compound, insoluble in water, was filtered, washed with water, and dried giving a white crystalline solid II (4.0 g, 10.3 mmol). Yield 73%. (Elemental analysis Calc. for $C_{20}H_{20}O_8$: C, 61.83, H, 5.19. Found: C, 61.91; H, 5.22%.)

^{1}H NMR (DMSO-d$_6$, ppm): 0.81 (t, 6H, CH$_3$); 1.25 (q, 4H, CH$_2$); 3.72 (q, 4H, CH$_2$); 4.00 (s, 4H broad, COOH); 7.37 (d, 4H *ortho* H and *para* H); 7.78 (q, 2H-*meta* H).

2.3.3. 3-[8-(2-Carboxy-propyl)-naphthalen-1-yl]-2-methyl-propionic acid (III)

Tetra acid II (4.0 g, 10.3 mmol) was placed in a round-bottomed flask together with 25 cm^3 of HCl (1:1) and stirred at 80 °C until CO$_2$ evolution ended. Then the product was filtered, washed and dried giving a white solid III, (2.9 g, 9.7 mmol). Yield 94%. Melting point: 210–211 °C. (Elemental analysis Calc. for $C_{18}H_{20}O_4$: C, 71.98; H, 6.71. Found: C 71.60; H, 6.71%.)

^{1}H NMR (DMSO, ppm) δ 1.21 (t, 6H, CH$_3$); 2.52 broad (t, 4H, CH$_2$); 3.45 broad (t, 2H, CH); 4.00 broad (H of COOH); 7.37 (d, 4H *ortho H* and *para* H); 7.78 (q, 2H *meta* H).

2.3.4. 2,9-Dimethyl-1,2,9,10-tetrahydro-dicyclopenta-[a,h]naphthalene-3,8-dione (IV)

A large excess of polyphosphoric acid (75 g) and III (2.9 g, 9.6 mmol) were placed in a 1 l round-bottomed flask fitted with a mechanical stirrer and a nitrogen inlet. The mixture was stirred vigorously under nitrogen at 80 °C for 2 h. Then it was poured into a mixture of 500 g of ice in 2 l of H$_2$O. The resulting yellow precipitate was filtered, washed with water and dried. The solid was dissolved in chloroform (200 cm^3), filtered and the solvent removed under vacuum to afford a yellow colored solid, essentially pure mixture of two isomers of IV in the 1:1 proportion (1.86 g, 7.09 mmol). Yield 74%. It can also be purified by chromatography on silica gel (50 g, ether, dichloromethane 3.7 v/v) affording 1.86 g of IV. Yield: 74% (Elemental analysis Calc. for $C_{18}H_{16}O_2$: C, 81.79; H, 6.10. Found: C, 81.91; H, 5.91%.)

^{1}H NMR (CDCl$_3$, ppm): isomer 1: δ 1.43 (d, J^3 = 7.38 Hz, 6H, CH$_3$); 2.87 (qdd, J^3 = 7.44 Hz, J^3 = 2.86 Hz, J^3 = 1.72 Hz, 2H, CH); 3.30 (dd, J^2 = 17.72 Hz, J^3 = 2.86 Hz, 2H, CH$_2$); 4.03 (d, J^1 = 17.72 Hz, 2H, CH$_2$); 7.90 (s, 4H, Ar–CH). ^{1}H NMR (CDCl$_3$, ppm): isomer 2: δ 1.43 (d, J^3 = 7.38 Hz, 6H, CH$_3$); 2.90 (qdd, J^3 = 7.44 Hz, J^3 = 3.06 Hz, J^3 = 1.75 Hz, 2H, CH); 3.31 (dd, J^2 = 17.72 Hz,

J^3 = 3.06 Hz, 2H, CH$_2$); 4.07 (d, J^1 = 17.72 Hz, 2H, CH$_2$); 7.90 (s, 4 H, Ar–CH). ^{13}C{^{1}H} NMR (CDCl$_3$, ppm): δ 15.6 (CH$_3$), 32.9 (CH$_2$), 42.8 (CH), 125.6 (quaternary), 126.6 (quaternary), 130.6 (quaternary), 130.7 (quaternary), 134.5 (quaternary), 145.4 (quaternary) and 209 (C=O, quaternary). IR(KBr): 1706 cm^{-1} (ν(C=O)). Mass Spectrum (EI, *m/z*, %): 264 (M$^+$, 100%), 265 (M$^+$ + 1, 19.7%), 266 (M$^+$ + 2, 2.3%).

2.3.5. 2,9-Dimethyl-1,2,3,8,9,10-hexahydro-dicyclopenta-[a,h]naphthalene-3,8-diol (V)

To LiAlH$_4$ (0.72 g, 18.90 mmol) in 25 cm^3 of diethyl-ether placed in a round-bottomed flask (250 cm^3) was added slowly with stirring at room temperature IV (1.86 g, 7.09 mmol) in 25 cm^3 diethylether. After 3 h of stirring and reflux, the mixture was cooled to 0 °C and a solution of HCl (18%, 100 cm^3) was added. The ether layer was separated and the water layer was extracted twice with 100 cm^3 of ether. The ether layer and extracts were combined and dried under vacuum to give a white solid (1.75 g, 6.6 mmol). Yield 94%. (Elemental analysis Calc. for $C_{18}H_{18}O_2$: C, 80.59; H, 7.51. Found: C, 80.12; H, 7.30%.)

^{1}H NMR (DMSO, ppm): δ 1.25 (t, 6H, CH$_3$); 2.20 (q, 2H, CH); 4.49 (s, 2H, OH); 5.18 (broad t, enolic H); 7.45 and 7.72, doublet (aromatic protons, AB system). IR (KBr): 3344.5 cm^{-1} (–OH). Mass spectrum (EI, *m/e*, %.): 268 (M$^+$, 100%), 269 (M$^+$ + 1, 19.8%), 270 (M$^+$ + 2, 2.2%).

2.3.6. 2,9-Dimethyl-1,10-dihydro-dicyclopenta[a,h]-naphthalene (VI)

The diol (V), (1.70 g, 6.4 mmol) was stirred for 1 h under nitrogen with *p*-toluene sulphonic acid (20 mg) in 100 cm^3 of benzene at 75 °C. Then, the solution was cooled to 0 °C and filtered to remove unreacted V. The organic phase was washed with water and dried over MgSO$_4$ for 18 h. After evaporation of the solvent in vacuum, crude VI obtained as a yellow powder was recrystallized from pentane (1.2 g, 5.2 mmol). Yield 81%. (Elemental analysis Calc. for $C_{18}H_{16}$: C, 93.06; H, 6.94. Found: C, 93.08; H, 6.87%.)

^{1}H NMR (CDCl3): δ (d, J^4 = 1.31 Hz, 6H, CH3); 3.60 (s, 4H, CH2); 6.66 (q, J^4 = 1.31 Hz, 2H, =CH); 7.42 (d, J^3 = 8.37 Hz, 2H, CH Ar); 7.49 (d, J^3 = 8.37 Hz, 2H, CH Ar). ^{13}C{^{1}H} NMR(C$_6$D$_6$): 25.2 (CH$_3$), 41.5 (CH$_2$), 122.4 (quaternary), 126.5 (quaternary), 128.0 (quaternary), 128.5 (quaternary), 130.5 (quaternary), 132.1 (quaternary), 135.0 (quaternary) and 145.9 (quaternary). Mass spectrum (EI, *m/e*, %): 232 (M$^+$, 100%), 233 (M$^+$ + 1, 19.7%), 234 (M$^+$ + 2, 1.8%).

2.3.7. Cp*Fe(2,9-dimethyl-dicyclopenta[a,h]-naphthalenylene)FeCp* (1)

Fe(acac)$_2$ (0.86 g, 3.4 mmol) was dissolved in THF (30 cm^3) and cooled to −78 °C. A suspension of Cp*Li

(0.48 g, 3.4 mmol) was then added to the mixture and subsequently warmed to room temperature. In another flask, a hexane solution of *n*-butyl lithium (1.6 M, 2.1 cm^3, 3.4 mmol) was added dropwise to 2,9-di-methyl-1,10-dihydro-dicyclopenta[*a,h*]naphthalene (**VI**) (0.5 g, 1.7 mmol) dissolved in THF (20 cm^3) at −78 °C, to form the dilithium salt. This mixture was allowed to warm to room temperature before the Cp*Fe(acac) solution was added with stirring, at −78 °C. The mixture was warmed to room temperature and stirred for 2 h. Solvent was removed under vacuum and the product was extracted with toluene until the extraction became colorless. The combined extracts were put together and the solvent evaporated to dryness. The residue was dissolved in pentane (10 cm^3) and the solution cooled to −78 °C. The precipitated was filtered and dried, yielding 0.75 g (1.22 mmol, 71%) of a red microcrystalline product, which was recrystallised from toluene. (Elemental analysis Calc. for C$_{38}$H$_{46}$Fe$_2$: C, 74.52; H 7.43%. Found: C, 74.18; H, 7.43%).

^{1}H NMR, (C$_6$D$_6$, ppm) δ 1.44 (s, 30H, Cp*); 2.02 (s, 6H, CH$_3$); 4.07 (s, 2H, Cp ring); 4.83 (s, 2H, Cp ring); 7.29 (d, J^3 = 8.86 Hz, 2H, Ar). Mass spectrum (EI, *m/z*, %): 614 (M$^+$, 100%), 615 (M$^+$ + 1, 41.6%), 612 (M$^+$ + 2, 12.7%), 616 (M$^+$ + 4, 10.4%), 617 (M$^+$ + 5, 1.1%).

2.3.8. [Cp*Fe(2,9-dimethyl-dicyclopenta[a,h]-naphthalenylene)FeCp*]$^+$BF$_4^-$, (2)

Complex **1** (250 mg 0.4 mmol) dissolved in 20 cm^3 THF was added to [FeCp$_2$]$^+$[BF$_4$]$^-$ (0.11 g 0.4 mmol) and the mixture was stirred at rt for 4 h resulting in the formation of a blue precipitate. The mixture was filtered and the solid was washed with diethylether and dried under vacuum. The crude solid was recrystallized by slow diffusion of diethylether into a concentrated DCM solution of **2**. Blue crystals appeared within 24 h. The crystals were filtered, washed with diethylether, and dried under vacuum, the yield of **2** was 0.16 g, (0.19 mmol, yield 48%). (Elemental analysis Calc. for C$_{38}$H$_{46}$Fe$_2$BF$_4$: C, 65.08; H, 6.60%.)

3. Results and discussion

3.1. Ligand synthesis

Since for the synthesis of the binuclear derivatives of iron, we required a reasonable amount of the ligand 2,9-dimethyl-1,10-dihydro-dicyclopenta[*a,h*]naphthalene and according to the procedure described by Katz and coworkers [4] the yield in the step of the reduction of the polycyclic diketone for us were poor (8–10%), we tried instead of this to prepare the dialkyl substituted derivative, 2,9-dimethyl-1,10-dihydro-dicyclopenta[*a,h*]-naphthalene. The adopted route is shown in Scheme 1.

It was based on a modification of previously described preparations of partially alkylated dihydro-s-indacenes [13] and dicyclopenta[*a,f*]naphthalene [14].

The alkylation of methyl malonic ester produced the tetra ester **I** in almost quantitative yield. Saponification and decarboxylation produced moderate yields of the diacid, 3-[8-(2-carboxy-propyl)-naphthalen-1-yl]-2-methyl-propionic acid (**III**). Upon treatment with polyphosphoric acid, the diacid underwent a double cyclization to give the corresponding polycyclic diketone **IV**. Proton NMR spectroscopy revealed the presence of two isomers in an approximate ratio of 1:1. In contrast to the 1,2,9,10-tetrahydro-dicyclopenta[*a,h*]naphthalene-3,8-dione, reported by Katz [4], in which case the reduction with LiAlH$_4$ the diketone was recovered after the work-up, we found that the diol **V**, could be obtained in almost quantitative yield. This difference is possibly due to the presence of the methyl group, which inhibits the formation of the enol form. Since compound **V** undergoes a spontaneous partial dehydration under the experimental conditions used for its preparation, it was obtained as a mixture of alcohol and ligand, and no further attempts were made to purify in order to keep substance losses at a minimum. Further dehydration of **V** lead to hydrocarbon **VI** (H$_2$L). The ^{1}H and ^{13}C NMR spectra show this hydrocarbon to be homogeneous and is in accord with the structure pictured. Starting from 1,8-di(bromomethyl) naphthalene the overall yields of these five steps was around 45%. This new substituted ligand shows a high solubility in most common organic solvents like pentane, hexane and aromatics.

3.2. Synthesis and characterization of [{(η^5-C$_5$Me$_5$)-Fe}$_2$L] (1)

Our synthetic strategy for the preparation of the biferrocene, [{(η^5-C$_5$Me$_5$)Fe}$_2$L] (**1**) was salt-elimination, utilizing the reaction of the dianion of the ligand [(Li$^+$)$_2$(L^{2-})] prepared in situ, with two moles of (η^5-C$_5$Me$_5$)Fe(acac) as shown in Scheme 2. The reaction afforded a red solution from which air sensitive red crystals of **1** were obtained after recrystallization from pentane. NMR spectroscopy showed only a single isomer to be present; X-ray structure determination revealed this was the *anti* isomer.

3.3. Synthesis and characterization of [{(η^5-C$_5$Me$_5$)-Fe}$_2$L]$^+$[BF$_4$]$^-$ (2)

Treatment of one equivalent of a THF solution of **1** with one equivalent of ferrocenium tetrafluoroborate gave, after washing with diethylether in order to remove all ferrocene, a dark precipitate of the salt [{(η$_5$-C$_5$Me$_5$)Fe}$_2$L]$^+$[BF$_4$]$^-$ (**2**). Blue dark paramagnetic air-sensitive microcrystals of **2** were obtained after recrystallization of the solid by slow diffusion of diethyl
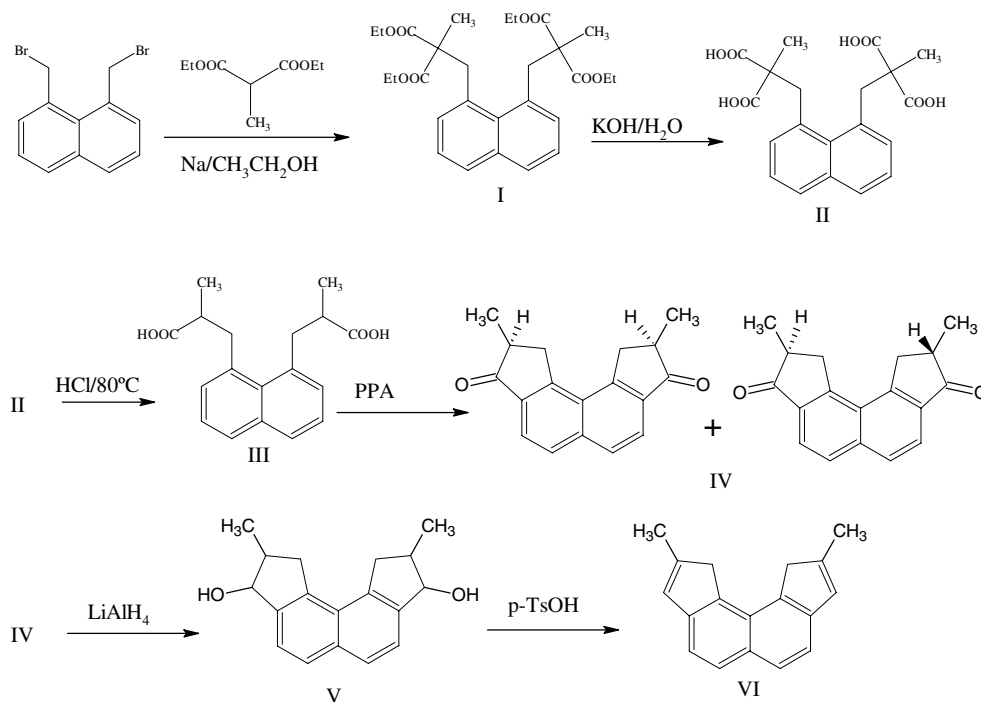
Scheme 1. Preparation of ligand.
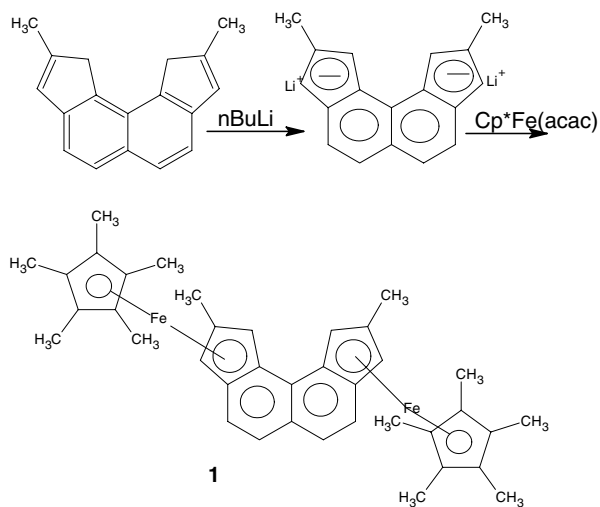
Scheme 2. Synthesis of the organometallic derivatives.

ether into a concentrated dichloromethane (DCM) solution of the salt.

3.4. Electrochemical characterization of $[\{(\eta^5\text{-}C_5Me_5)\text{-}Fe\}_2L]$ (1)

Cyclic voltammetry studies of **1** were carried out in dichloromethane solvent with tetrabutylammonium tetrafluoroborate as a supporting electrolyte. The cyclic voltammograms present a first reversible redox couple and a second quasi-reversible couple (see Fig. 2). The values of the potential change slightly with the

scan rates. At 50 mV s^{-1}, the oxidations (E_{pa}) occur at E_{pa1} = 65 and E_{pa2} = 413 mV, respectively, versus SCE. Controlled potential electrolysis at 333 mV allowed us to determine that one equivalent of charge per mole of complex has been transferred in this first redox process.

The initial dark red solution changes to a violet color solution. Reverse electrolysis re-established the initial
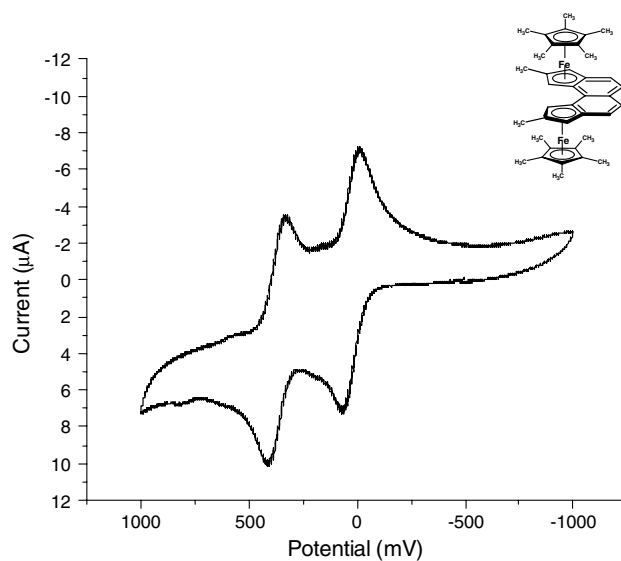

Fig. 2. Cyclic voltammogram of [Cp*Fe(2,9-dimethyl-1,10-dihydro-dicyclopenta[*a,h*]naphthalene)FeCp*] complex.

Table 1
Hyperfine parameters for the fitting of the Mössbauer spectra of compounds **1** (80 K) and **2** (several temperatures)

Compound	Temperature (K)	Site	δ_{Fe} (mm s$^-$)	ΔE_q (mm s$^-$)	Γ (mm s$^-$)	Area ± 2%
Complex **1**	80	Fe^{2+}	0.520(2)	2.42(2)	0.28(1)	84
		Fe^{3+}	0.431(2)	0.70(2)	0.49(2)	16
Complex **2**	80	Fe^{2+}	0.513(2)	2.052(2)	0.314(4)	49
		Fe^{3+}	0.506(2)	0.665(2)	0.283(4)	51
	120	Fe^{2+}	0.508(8)	2.055(9)	0.31(2)	47
		Fe^{3+}	0.500(6)	0.68(1)	0.29(1)	53
	200	Fe^{2+}	0.472(4)	2.018(6)	0.33(1)	45
		Fe^{3+}	0.473(2)	0.678(6)	0.301(8)	55
	300	Fe^{2+}	0.434(4)	2.02(1)	0.36(3)	41
		Fe^{3+}	0.419(6)	0.68(1)	0.35(2)	59
	80 (after heating)	Fe^{2+}	0.513(2)	2.073(4)	0.319(6)	48
		Fe^{3+}	0.506(2)	0.664(2)	0.301(4)	52

δ_{Fe}, ΔE_q and Γ are the isomer shift (relative to metallic iron), quadrupolar splitting and the full width at half maximum, respectively. The area represents the Mössbauer fraction of each sub-spectra in relative percentage. The errors are given within brackets and correspond to the last digit.

neutral binuclear complex. When the complex is electro-lyzed at 680 mV, the complex is completely oxidized and the solution becomes blue.
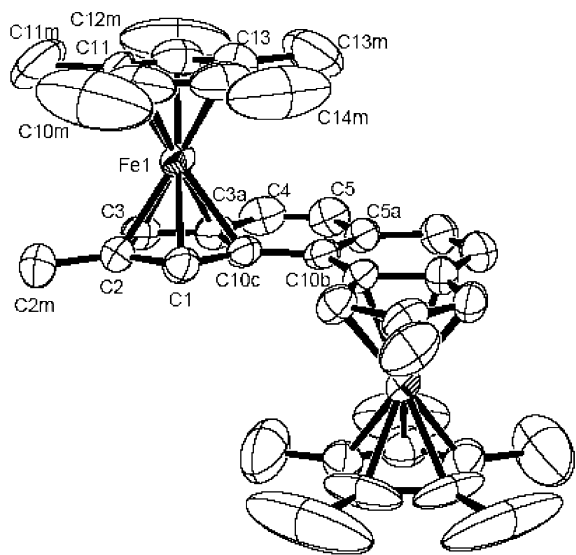
Fig. 3. Crystal structure diagram of [Cp*Fe(2,9-dimethyl-1,10-dihydro-dicyclopenta[*a,h*]naphthalene)FeCp*] complex (**1**) showing the numbering schema used. Displacement ellipsoids drawn at 40% level. Hydrogen atoms are not shown for clarity.

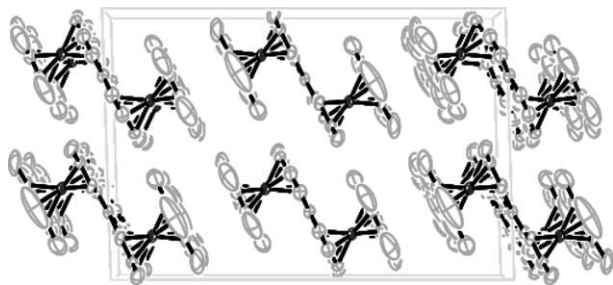Fig. 4. Crystal structure of a unit cell of [Cp*Fe(2,9-dimethyl-1,10-dihydro-dicyclopenta[*a,h*]naphthalene)FeCp*] complex (**1**).
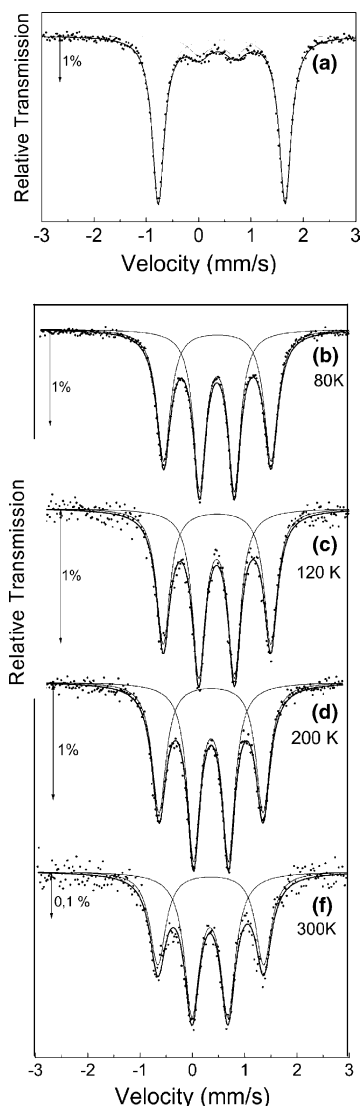

Fig. 5. (a) Mössbauer spectrum of [Cp*Fe(2,9-dimethyl-1,10-dihydro-dicyclopenta[*a,h*]naphthalene)FeCp*] complex (**1**) at 80 K. (b–f) Mössbauer spectra of [Cp*Fe(2,9-dimethyl-1,10-dihydro-dicyclopenta[*a, h*]naphthalene)FeCp*]$^+$BF$_4^-$ complex (**2**) at several temperatures.

Table 2
Crystal data and structure refinement for Ch4

Identification code	Ch4
Empirical formula	$C_{38}H_{44}Fe_2$
Formula weight	612.43
Temperature (K)	293(2)
Wavelength (Å)	0.71073
Crystal system	Monoclinic
Space group	$I2/a$
Unit cell dimensions	
a (Å)	15.030
b (Å)	8.613
c (Å)	23.921
α (°)	90
β (°)	92.01
γ (°)	90
Volume (Å^3)	3094.7
Z	4
Density (calculated) (Mg m^{-3})	1.314
Absorption coefficient (mm^{-1})	0.962
$F(0\,0\,0)$	1296
Crystal size (mm^3)	$0.40 \times 0.26 \times 0.09$
Theta range for data collection (°)	1.70–24.98
Index ranges	$-17 \leqslant h \leqslant 0,\ 0 \leqslant k \leqslant 10,$ $-28 \leqslant l \leqslant 28$
Reflections collected	2838
Independent reflections	2723 [$R_{int} = 0.0464$]
Completeness to theta = 24.98° (%)	99.9
Refinement method	Full-matrix least-squares on F^2
Data/restraints/parameters	2723/54/188
Goodness-of-fit on F^2	1.057
Final R indices [$I > 2\sigma(I)$]	$R_1 = 0.0801,\ wR_2 = 0.2002$
R indices (all data)	$R_1 = 0.1583,\ wR_2 = 0.2377$
Largest difference peak and hole (e Å^{-3})	0.732 and -0.443

The difference of potential (ΔE_{pa}) between the oxidation peaks was 348 mV. This value of ΔE indicates the moderate interaction between the iron atoms, characteristic of a class II compound of Robin and Day's classification [15]. On the other hand, both oxidized complexes are stable in the solution of DCM without oxygen. The first anodic process (E_{pa1}) presents a intensity current ratio equal to unity ($I_{pa1}/I_{pc1} = 1$), thus indicative of the reversibility of the process. Whereas in the second anodic process (E_{pa2}), the intensity current ratio presents a slight deviation from unity ($I_{pa2}/I_{pc2} = 1.18$).

A UV–Vis-NIR spectrum was recorded for the complex **2**. The mixed valence complex obtained by electrolysis in DCM presents an intervalence transfer band at 850 nm. This band is not present in the neutral complex and is not observed when the complex is oxidized twice. The same band is observed for the mixed valence complex prepared by chemical procedures. The position of intervalence transfer of complex **2** when recorded in acetonitrile and acetone shifts to 812 and 800 nm, respectively. The solvent dependence of this band is also a characteristic feature of complexes that belong to class **II**.

3.5. Crystallography

A suitable dark red flat crystal of **1** was selected for the single crystal X-ray diffraction experiment. Once glued at the tip of a glass fiber and mounted on an Enraf Nonius CAD4 diffractometer (graphite monochro-

Table 3
Atomic coordinates ($\times 10^4$) and equivalent isotropic displacement parameters (Å$^2 \times 10^3$) for Ch4

	x	y	Z	U(eq)
C(1)	3452(6)	2185(10)	4661(4)	48(2)
C(2)	4288(6)	2114(11)	4401(4)	53(2)
C(2M)	4782(7)	661(14)	4251(4)	77(3)
C(3)	4578(6)	3645(11)	4310(4)	51(2)
C(3A)	3957(6)	4672(11)	4529(4)	50(2)
C(4)	3922(7)	6365(12)	4558(4)	63(3)
C(5)	3232(7)	7055(11)	4776(4)	58(2)
C(5A)	2500	6197(14)	5000	44(3)
C(10B)	2500	4595(14)	5000	43(3)
C(10C)	3240(6)	3797(10)	4754(3)	42(2)
C(10)	2778(13)	1972(12)	3317(6)	110(5)
C(10M)	2670(20)	270(20)	3326(10)	276(14)
C(11)	3499(8)	2950(20)	3089(4)	99(5)
C(11M)	4289(13)	2310(40)	2815(6)	253(13)
C(12)	3247(8)	4430(15)	3164(4)	74(3)
C(12M)	3810(15)	5840(30)	2981(8)	218(12)
C(13)	2480(8)	4509(15)	3395(4)	72(3)
C(13M)	1976(14)	6000(20)	3539(7)	171(9)
C(14)	2166(8)	3097(18)	3511(4)	80(4)
C(14M)	1292(11)	2720(30)	3781(7)	201(11)
Fe(1)	3370(1)	3306(1)	3908(1)	42(1)

U(eq) is defined as one third of the trace of the orthogonalized U^{ij} tensor.

Table 4
Bond lengths (Å) and angles (°) for Ch4

C(1)–C(2)	1.422(12)
C(1)–C(10C)	1.443(12)
C(1)–Fe(1)	2.043(8)
C(2)–C(3)	1.409(13)
C(2)–C(2M)	1.505(13)
C(2)–Fe(1)	2.057(9)
C(3)–C(3A)	1.400(12)
C(3)–Fe(1)	2.045(9)
C(3A)–C(10C)	1.435(11)
C(3A)–C(4)	1.461(13)
C(3A)–Fe(1)	2.067(9)
C(4)–C(5)	1.318(14)
C(5)–C(5A)	1.444(11)
C(5A)–C(10B)	1.380(16)
C(5A)–C(5)#1	1.444(11)
C(10B)–C(10C)	1.450(10)
C(10B)–C(10C)#1	1.450(10)
C(10C)–Fe(1)	2.082(8)
C(10)–C(14)	1.426(19)
C(10)–C(10M)	1.47(2)
C(10)–C(11)	1.49(2)
C(10)–Fe(1)	2.006(10)
C(11)–C(12)	1.346(19)
C(11)–C(11M)	1.482(17)
C(11)–Fe(1)	2.000(10)
C(12)–C(13)	1.297(15)
C(12)–C(12M)	1.549(19)
C(12)–Fe(1)	2.030(10)
C(13)–C(14)	1.338(16)
C(13)–C(13M)	1.537(17)
C(13)–Fe(1)	2.063(11)
C(14)–C(14M)	1.518(18)
C(14)–Fe(1)	2.022(10)
C(2)–C(1)–C(10C)	108.2(8)
C(2)–C(1)–Fe(1)	70.3(5)
C(10C)–C(1)–Fe(1)	71.0(5)
C(3)–C(2)–C(1)	108.1(8)
C(3)–C(2)–C(2M)	125.7(8)
C(1)–C(2)–C(2M)	126.2(9)
C(3)–C(2)–Fe(1)	69.5(5)
C(1)–C(2)–Fe(1)	69.1(5)
C(2M)–C(2)–Fe(1)	127.2(7)
C(3A)–C(3)–C(2)	108.6(8)
C(3A)–C(3)–Fe(1)	70.9(5)
C(2)–C(3)–Fe(1)	70.4(5)
C(3)–C(3A)–C(10C)	109.1(8)
C(3)–C(3A)–C(4)	132.4(9)
C(10C)–C(3A)–C(4)	118.5(9)
C(3)–C(3A)–Fe(1)	69.3(5)
C(10C)–C(3A)–Fe(1)	70.3(5)
C(4)–C(3A)–Fe(1)	126.0(7)
C(5)–C(4)–C(3A)	120.0(9)
C(4)–C(5)–C(5A)	122.4(9)
C(10B)–C(5A)–C(5)	120.8(6)
C(10B)–C(5A)–C(5)#1	120.8(6)
C(5)–C(5A)–C(5)#1	118.4(11)
C(5A)–C(10B)–C(10C)	118.3(5)
C(5A)–C(10B)–C(10C)#1	118.3(5)
C(10C)–C(10B)–C(10C)#1	123.4(11)
C(3A)–C(10C)–C(1)	105.9(8)
C(3A)–C(10C)–C(10B)	120.0(8)
C(1)–C(10C)–C(10B)	134.0(8)
C(3A)–C(10C)–Fe(1)	69.2(5)

Table 4 (*continued*)

C(1)–C(10C)–Fe(1)	68.1(5)
C(10B)–C(10C)–Fe(1)	126.2(5)
C(14)–C(10)–C(10M)	127(2)
C(14)–C(10)–C(11)	102.9(9)
C(10M)–C(10)–C(11)	130(2)
C(14)–C(10)–Fe(1)	69.9(6)
C(10M)–C(10)–Fe(1)	127.2(10)
C(11)–C(10)–Fe(1)	68.0(6)
C(12)–C(11)–C(11M)	130(2)
C(12)–C(11)–C(10)	105.9(10)
C(11M)–C(11)–C(10)	124(2)
C(12)–C(11)–Fe(1)	71.7(6)
C(11M)–C(11)–Fe(1)	126.7(9)
C(10)–C(11)–Fe(1)	68.4(6)
C(13)–C(12)–C(11)	111.4(12)
C(13)–C(12)–C(12M)	125.6(16)
C(11)–C(12)–C(12M)	123.0(16)
C(13)–C(12)–Fe(1)	72.9(7)
C(11)–C(12)–Fe(1)	69.3(7)
C(12M)–C(12)–Fe(1)	125.9(9)
C(12)–C(13)–C(14)	111.5(12)
C(12)–C(13)–C(13M)	126.3(14)
C(14)–C(13)–C(13M)	122.2(14)
C(12)–C(13)–Fe(1)	70.1(7)
C(14)–C(13)–Fe(1)	69.2(7)
C(13M)–C(13)–Fe(1)	126.9(9)
C(13)–C(14)–C(10)	108.2(11)
C(13)–C(14)–C(14M)	126.8(17)
C(10)–C(14)–C(14M)	124.9(17)
C(13)–C(14)–Fe(1)	72.5(6)
C(10)–C(14)–Fe(1)	68.7(7)
C(14M)–C(14)–Fe(1)	126.4(8)
C(11)–Fe(1)–C(10)	43.6(6)
C(11)–Fe(1)–C(14)	69.0(5)
C(10)–Fe(1)–C(14)	41.5(6)
C(11)–Fe(1)–C(12)	39.0(5)
C(10)–Fe(1)–C(12)	68.3(5)
C(14)–Fe(1)–C(12)	65.0(4)
C(11)–Fe(1)–C(1)	141.8(6)
C(10)–Fe(1)–C(1)	111.3(5)
C(14)–Fe(1)–C(1)	113.4(4)
C(12)–Fe(1)–C(1)	178.2(4)
C(11)–Fe(1)–C(3)	111.5(5)
C(10)–Fe(1)–C(3)	141.0(6)
C(14)–Fe(1)–C(3)	176.9(5)
C(12)–Fe(1)–C(3)	113.3(4)
C(1)–Fe(1)–C(3)	68.2(4)
C(11)–Fe(1)–C(2)	113.5(4)
C(10)–Fe(1)–C(2)	113.0(5)
C(14)–Fe(1)–C(2)	142.7(5)
C(12)–Fe(1)–C(2)	141.2(4)
C(1)–Fe(1)–C(2)	40.6(3)
C(3)–Fe(1)–C(2)	40.2(4)
C(11)–Fe(1)–C(13)	65.0(5)
C(10)–Fe(1)–C(13)	66.8(5)
C(14)–Fe(1)–C(13)	38.2(5)
C(12)–Fe(1)–C(13)	36.9(4)
C(1)–Fe(1)–C(13)	141.3(4)
C(3)–Fe(1)–C(13)	139.0(5)
C(2)–Fe(1)–C(13)	178.1(4)
C(11)–Fe(1)–C(3A)	137.5(6)
C(10)–Fe(1)–C(3A)	178.8(7)
C(14)–Fe(1)–C(3A)	137.8(5)
C(12)–Fe(1)–C(3A)	112.5(4)

Table 4 (*continued*)

C(1)–Fe(1)–C(3A)	68.0(4)
C(3)–Fe(1)–C(3A)	39.8(3)
C(2)–Fe(1)–C(3A)	67.2(4)
C(13)–Fe(1)–C(3A)	113.2(4)
C(11)–Fe(1)–C(10C)	177.2(6)
C(10)–Fe(1)–C(10C)	138.3(6)
C(14)–Fe(1)–C(10C)	111.2(4)
C(12)–Fe(1)–C(10C)	138.3(5)
C(1)–Fe(1)–C(10C)	40.9(3)
C(3)–Fe(1)–C(10C)	68.1(3)
C(2)–Fe(1)–C(10C)	68.2(3)
C(13)–Fe(1)–C(10C)	113.3(4)
C(3A)–Fe(1)–C(10C)	40.5(3)

Symmetry transformations used to generate equivalent atoms: #1 $-x + 1/2, y, -z + 1$.

mated Mo Kα radiation), the cell parameters were obtained by indexing 25 randomly searched reflections (see Tables 2–5 for crystal data). Data were collected up to $2\vartheta = 50°$ in the $\omega - 2\vartheta$ scan mode resulting in 2838 reflections. Several absorption corrections were essayed (PSI-scan, DIFABS) without improving the initial data, so only Lorentz and polarisation corrections were applied. The space group was determined as $I2/a$ with $Z = 4$. The structural resolution procedure was made using the WINGX [16] package. Solving for structure factor phases was performed by SIR2002 [17] and the full-matrix refinement, by SHELXL97 [18]. The asymmetric unit give rise to the complete molecule by the application of a binary axis, being C5a and C10b just sitting on this axis. Non-H atoms were refined anisotropically and H-atoms were introduced in calculated positions and refined riding on their parent

atoms. A restraint was applied on some Cp* atoms to avoid too elongated ellipsoids. The final R indices were for $I > 2\sigma(I)$: $R_1 = 0.0801$, $wR_2 = 0.2002$, and for all data: $R_1 = 0.1583$, $wR_2 = 0.2377$. The largest difference Fourier peak and hole were 0.732 and -0.443 e Å^{-3}. Crystallographic data have been deposited with the CCDC as supplementary material with the deposition number 244506 [19] (see Fig. 3).

The range of Fe–C distances is 2.000–2.083 Å, with an average value of 2.0416 Å. The distance between Fe1 and Cg1 (centred of the C1, C2, C3, C3a, C10c ring) is 1.666(4) Å and the corresponding ring slippage (distance between the perpendicular projection of Fe1 on the ring least-squares plane and the ring centroid) is 0.024 Å. The distance between Fe1 and Cg2 (centroid of the C10, C11, C12, C13, C14 ring) is 1.650(5) Å and the Cp* ring slippage is 0.094 Å. The axial thermal vibration of the Cp* group appears as off-centred, as has been usually observed in other numerous cases [6,11]. A view of the unit cell along **b** (see Fig. 4) shows the crystal packing.

3.6. Mössbauer spectroscopy characterization of compounds 1 and 2

Mössbauer spectroscopy is a local probe method and consequently very sensitive to the iron electronic oxidation state and to its crystallographic environment.

The neutral compound, **1**, was measured at 80 K while the mixed-valence compound **2** was measured at several temperatures (80, 120, 200 and 300 K). Fig. 5 shows the Mössbauer spectra of the two compounds. Hyperfine parameters resulting from the fitted spectra are gathered in Table 1.

Table 5
Anisotropic displacement parameters (Å$^2 \times 10^3$) for Ch4

	U^{11}	U^{22}	U^{33}	U^{23}	U^{13}	U^{12}
C(1)	61(6)	42(5)	42(5)	4(4)	8(4)	4(4)
C(2)	56(5)	63(7)	41(5)	2(4)	8(4)	16(5)
C(2M)	83(8)	86(8)	63(6)	3(6)	19(6)	35(7)
C(3)	39(5)	69(7)	45(5)	9(5)	5(4)	−7(5)
C(3A)	43(5)	61(6)	46(5)	6(5)	3(4)	−10(5)
C(4)	72(7)	58(7)	58(6)	4(5)	1(5)	−22(5)
C(5)	73(6)	40(5)	60(6)	2(4)	3(5)	−9(5)
C(5A)	56(7)	35(7)	42(6)	0	3(6)	0
C(10B)	53(7)	45(7)	30(6)	0	0(5)	0
C(10C)	49(5)	45(5)	32(4)	3(4)	5(4)	1(4)
C(10)	209(14)	29(6)	85(8)	−10(6)	−82(9)	2(8)
C(10M)	500(30)	77(12)	230(20)	−24(14)	−240(20)	−2(18)
C(11)	78(7)	188(14)	31(5)	−30(7)	0(5)	65(9)
C(11M)	195(17)	500(30)	59(9)	−75(15)	−6(10)	200(20)
C(12)	71(7)	97(10)	54(6)	20(6)	−2(6)	−12(7)
C(12M)	250(20)	260(20)	139(15)	129(16)	−84(15)	−150(20)
C(13)	71(7)	85(9)	59(6)	2(6)	−8(6)	10(7)
C(13M)	230(20)	147(15)	128(14)	−35(12)	−86(14)	117(15)
C(14)	72(7)	115(11)	50(6)	13(7)	−13(5)	−37(8)
C(14M)	112(12)	390(30)	98(11)	68(16)	−18(9)	−116(17)
Fe(1)	45(1)	48(1)	33(1)	2(1)	6(1)	−1(1)

The anisotropic displacement factor exponent takes the form: $-2\pi^2[h^2a^{*2}U^{11} + \cdots + 2hka^*b^*U^{12}]$.

The spectrum of the neutral compound (**1**) consists of a Fe^{2+} site (84% of the resonant Mössbauer area) with the hyperfine values characteristic of a ferrocene-based compound. The residual 16% of the resonant area has typical parameters of a Fe^{3+} site and, considering the extreme oxygen avidity of these compounds, it is probably a result of a partial oxidation of the compound during the sample preparation.

The spectra of the mixed valence compound (**2**) were fitted using two symmetrical doublets corresponding to the two-oxidation states (Fe^{2+} and Fe^{3+}). At 80 K the resonant area corresponding to the Fe^{2+} site is of 49% and it diminishes to a value of 41% at 300 K, indicating that by increasing the temperature the thermal activation promotes the electron to a close enough excited molecular orbital state. It is worth noting than the effect is reversible (see Table 1).

4. Conclusion

We have developed a convenient synthesis to a new dialkylated fused-ring ligand, 2,9-dimethyl-1,10-dihydrodicyclopenta[*a,h*]naphthalene (**VI**) (H$_2$L). We have proven that by means of salt elimination strategy, it is possible to obtain binuclear organometallic complexes which can be further oxidized either chemically or electrochemically to afford the corresponding mixed valence complex. From spectroscopic data and electrochemical studies, we can conclude that in the complex [Cp*Fe(2,9-dimethyl-1,10-dihydro-dicyclopenta[*a,h*]naphthalenylene)FeCp*]$^+$BF$_4^-$ (**2**) there is a moderate interaction between the metallic centers with a delocalization similar to the isomer [Cp*Fe(dicyclopenta-[*a,f*]naphthalenylene)FeCp*]$^+$BF$_4^-$ [11].

Acknowledgements

Appendix A. Supplementary data

References

[1] S. Barlow, D. O'Hare, Chem. Rev. 97 (1997) 637.
[2] T.J. Katz, J. Schulman, J. Am. Chem. Soc. 86 (1964) 3169.
[3] T.J. Katz, N. Action, J. McGinnis, J. Am. Chem. Soc. 9 (4) (1972) 6205.
[4] T.J. Katz, W. Sluzarek, J. Am. Chem. Soc. 101 (1979) 4259.
[5] W.L. Bell, C.J. Curtis, C.W. Eigenbrot, C.G. Pierpont, J.L. Robbins, J.C. Smart, Organometallics 6 (1987) 266.
[6] J.M. Manríquez, M.D. Ward, W. Reiff, J.C. Calabrese, N.L. Jones, P.J. Carrol, E. Bunel, J.S. Miller, J. Am. Chem. Soc. 117 (1995) 6182.
[7] S. Barlow, D. O'Hare, Organometallics 15 (1996) 3483.
[8] S. Barlow, D.R. Cary, M. Jdrewitt, D. O'Hare, J. Chem. Soc., Dalton Trans. (1997) 3867.
[9] D.R. Cary, C. Gwebster, M.J. Drewitt, S. Barlow, J.C. Green, D. O'Hare, Chem. Commun. (1997) 953.
[10] D.R Cary, J.C. Green, D. O'Hare, Angew. Chem. Int., Ed. Engl. 36 (1997) 2618.
[11] G. Alfonso, I. Chávez, V. Arancibia, J.M. Manríquez, M.T. Garland, A. Roig, E. Molins, R.F. Baggio, J. Orgmet. Chem. 620 (2001) 32, and the references therein.
[12] Emilio E. Bunel, Luis Valle, Juan M. Manriquez, Organometallics 4 (1985) 1680.
[13] M.R. Dahrouch, P. Jara, L. Mandez, Y. Portilla, D. Abril, G. Alfonso, I. Chavez, J.M. Manríquez, M.R. Baudet, P. Riviere, A. Castel, J. Rouzaud, H. Gornitzka, Organometallics 20 (2001) 5591.
[14] R.S. Schneider, E.F. Ullman, Tetrahedron Lett. (1969) 3249.
[15] M.B. Robin, P. Day, Adv. Inorg. Radio. 10 (1967) 247.
[16] G.X. Win, L.J. Farrugia, J. Appl. Crystallogr. 32 (1999) 837–838.
[17] M.C. Burla, M. Camalli, B. Carrozzini, G.L. Cascarano, C. Giacovazzo, G. Polidori, R. Spagna, J. Appl. Crystallogr. 36 (2003) 1203.
[18] G.M. Sheldrick, SHELXL97: Programs for Crystal Structure Analysis (Release 97-2), Institüt für Anorganische Chemie der Universität, Tammanstrasse 4, D-3400 Göttingen, Germany, 1998.
[19] CCDC 244506 contains the supplementary crystallographic data for this paper. These data can be obtained free of charge via www.ccdc.cam.ac.uk/data_request/cif, by emailing data_request@ccdc.cam.ac.uk, or by contacting The Cambridge Crystallographic Data Centre, 12, Union Road, Cambridge CB2 1EZ, UK; fax: +44 1223 336033.